Pergamon

*Int. J. Solids Structures* Vol. 35, Nos 34–35, pp. 4905–4929, 1998

Printed in Great Britain
0020–7683/98/$—see front matter

PII: S0020–7683(98)00101–2

# POROELASTIC SOLUTIONS IN TRANSVERSELY ISOTROPIC MEDIA FOR WELLBORE AND CYLINDER

Y. ABOUSLEIMAN
Department of Civil Engineering, School of Engineering and Architecture,
The Lebanese American University, Byblos, Lebanon

and

L. CUI
Rock Mechanics Institute, The University of Oklahoma, Norman, Oklahoma 73019, U.S.A.

(*Received* 1 *September* 1997; *in revised form* 12 *February* 1998)

**Abstract**—This paper presents closed-form solutions for the pore pressures and stress fields for the inclined borehole and the cylinder, induced by boundary stress perturbation in an anisotropic poroelastic medium. The governing equations for the transversely isotropic poroelastic materials under the cylindrical coordinate system are presented. The solution for the inclined borehole, subjected to a three-dimensional far-field anisotropic stress field, is derived with the borehole generator coinciding with the material axis of symmetry; while the solutions for the cylinder are obtained under various loading conditions that are encountered in laboratory testing procedures. The analysis shows, in addition to the effect of time on stress and pore pressure variations, that poromechanical anisotropic material coefficients also play an important role in calculating the in-plane stress fields, which is not the case using the classical anisotropic theory of elasticity. © 1998 Elsevier Science Ltd. All rights reserved.

## 1. INTRODUCTION

The theory of anisotropic poroelasticity was formulated by Biot (1955), in an attempt to generalize consolidation theory. Later, Biot and Willis (1957) extended the theory to describe various poromechanical properties of an anisotropic fluid saturated medium. In their work, the outlined experimental procedures for the determination of the directional poromechanical properties are extremely difficult to achieve, if not impossible. Following the interpretation of Rice and Cleary (1976) of the poroelastic material constants, Thompson and Willis (1991) reformatted the anisotropic poroelastic constitutive relations, in which the parameters that appear are given explicitly in terms of drained (elastic) and undrained compliances, and the generalized tensors of Skempton's pore pressure coefficient, $B_{ij}$, and Biot's effective stress coefficient, $\alpha_{ij}$. Recently, these parameters have been cast in a practical model for laboratory measurement (Cui, 1995; Cheng, 1997).

With these latest developments in material characterizations, the application of the anisotropic poroelastic theory to engineering problems becomes more amenable. Although geomaterials exhibit many forms of anisotropy, closed-form solutions for anisotropic poroelasticity are almost non-existent in the literature. Recently, the transverse anisotropic poroelastic solutions for the one-dimensional consolidation (Cui *et al.*, 1996a) and the two-dimensional Mandel's problem (Abousleiman *et al.*, 1996a) were derived. These solutions may not find a wide range of engineering applications, but they can serve as benchmarks validating numerical algorithms such as the finite element method (Cui *et al.*, 1996b).

In this work we extend the transverse isotropic poroelastic solutions to the cases of the inclined borehole and cylinder geometries. Stability of wellbores in deep drilling remains one of the major problems in the oil and gas industry. The cylinder is the geometry most widely used in laboratory testing procedures for rocks and other geo-materials.

## 2. GOVERNING EQUATIONS

For the borehole and cylinder problems it is natural to use the cylindrical coordinate system to analyze the poromechanical behavior of such geometries exhibiting axial symmetry. We limit the formulations and solutions to the transverse isotropic case, keeping in mind that the extension to the orthotropic one (associated with the cylindrical coordinate system) is natural, only its application is limited because it is necessary to determine the 13 poromechanical coefficients needed. In the case of transverse isotropy where only eight poromechanical parameters are involved with the $z$-axis assigned as the axis of material rotational symmetry, stress–strain relations are presented below:

$$\begin{Bmatrix} \sigma_{rr} \\ \sigma_{\theta\theta} \\ \sigma_{zz} \\ \tau_{r\theta} \\ \tau_{\theta z} \\ \tau_{rz} \end{Bmatrix} = \begin{bmatrix} M_{11} & M_{12} & M_{13} & 0 & 0 & 0 \\ M_{12} & M_{11} & M_{13} & 0 & 0 & 0 \\ M_{13} & M_{13} & M_{33} & 0 & 0 & 0 \\ 0 & 0 & 0 & M_{44} & 0 & 0 \\ 0 & 0 & 0 & 0 & M_{55} & 0 \\ 0 & 0 & 0 & 0 & 0 & M_{55} \end{bmatrix} \begin{Bmatrix} \varepsilon_{rr} \\ \varepsilon_{\theta\theta} \\ \varepsilon_{zz} \\ \gamma_{r\theta} \\ \gamma_{\theta z} \\ \gamma_{rz} \end{Bmatrix} - \begin{Bmatrix} \alpha \\ \alpha \\ \alpha' \\ 0 \\ 0 \\ 0 \end{Bmatrix} p. \tag{1}$$

In the above, $\varepsilon_{ii}$ and $\gamma_{ij}$ and $\sigma_{ii}$ and $\tau_{ij}$ are strain components and total stress components in the cylindrical coordinate system, respectively; $p$ is the pore pressure, $\alpha$ and $\alpha'$ are Biot's effective stress coefficients in the isotropic plane ($r$–$\theta$ plane) and in the $z$-direction, respectively; and $M_{ij}$ are components of the drained elastic modulus matrix given by:

$$M_{11} = \frac{E(E' - Ev'^2)}{(1+v)(E' - E'v - 2Ev'^2)} \tag{2a}$$

$$M_{12} = \frac{E(E'v + Ev'^2)}{(1+v)(E' - E'v - 2Ev'^2)} \tag{2b}$$

$$M_{13} = \frac{EE'v'}{E' - E'v - 2Ev'^2} \tag{2c}$$

$$M_{33} = \frac{E'^2(1-v)}{E' - E'v - 2Ev'^2} \tag{2d}$$

$$M_{44} = G = \frac{M_{11} - M_{12}}{2} = \frac{E}{2(1+v)} \tag{2e}$$

$$M_{55} = G' \tag{2f}$$

in which $E$ and $v$ are drained Young's modulus and Poisson's ratio in the isotropic plane, $E'$ and $v'$ are similar quantities related to the direction of the axis of symmetry, and $G'$ is the shear modulus related to the direction of the axis of symmetry.

The fluid volumetric variation relation for the transversely isotropic material may be written as:

$$\zeta = \frac{p}{M} + \alpha\varepsilon_{rr} + \alpha\varepsilon_{\theta\theta} + \alpha'\varepsilon_{zz} \tag{3}$$

where $\zeta$ is the variation of fluid content per unit reference volume, and $M$ is Biot's modulus.

It is noted that unlike elasticity, except for the permeability, eight material properties are required to define a transversely isotropic poroelastic material, such as those mentioned above: $E$, $E'$, $v$, $v'$, $G'$, $\alpha$, $\alpha'$ and $M$. However, they need not necessarily be measured directly. They can be determined from other parameters which are more convenient to measure in

the laboratory. For example, the poroelastic properties under undrained conditions are probably easier to be measured. A set of relations between the material properties adopted previously and the material properties related to the undrained state is listed below (see Cui, 1995; Cheng, 1997):

$$M_{11} = M^{u}_{11} - \alpha^2 M \tag{4a}$$

$$M_{12} = M^{u}_{12} - \alpha^2 M \tag{4b}$$

$$M_{13} = M^{u}_{13} - \alpha\alpha' M \tag{4c}$$

$$M_{33} = M^{u}_{33} - \alpha'^2 M \tag{4d}$$

$$\alpha = \frac{1}{3M}[B(M^{u}_{11} + M^{u}_{12}) + B' M^{u}_{13}] \tag{4e}$$

$$\alpha' = \frac{1}{3M}(2BM^{u}_{13} + B' M^{u}_{33}) \tag{4f}$$

where the superscript, u, indicates the undrained state; $M^{u}_{ij}$ are the elements of the undrained elastic matrix and can be expressed in terms of the undrained Young's moduli and Poisson's ratios by eqns (2); $B$ and $B'$ are, respectively, Skempton's coefficients in the isotropic plane and in the direction of the axis of elastic symmetry. The relation between variations of pore pressure and total stresses at the undrained state is defined through the Skempton's coefficients:

$$p^{u} = -\tfrac{1}{3}(B\sigma^{u}_{rr} + B\sigma^{u}_{\theta\theta} + B'\sigma^{u}_{zz}). \tag{5}$$

It is assumed that the material is homogeneous, the boundary conditions do not vary along the $z$-axis, and the depth of the domain in the $z$-direction is infinitely long or much greater than the cross-sectional geometry; hence, the generalized plane strain (or complete plane strain) condition manifests itself (Abousleiman *et al.*, 1996b; Cui *et al.*, 1997b). The generalized plane strain condition results in that all stress and strain components, and the pore pressure are $z$-independent; therefore, leading to the following governing equations.

Equilibrium equations

$$\frac{\partial \sigma_{rr}}{\partial r} + \frac{1}{r}\frac{\partial \tau_{\theta r}}{\partial \theta} + \frac{\sigma_{rr} - \sigma_{\theta\theta}}{r} = 0 \tag{6a}$$

$$\frac{\partial \tau_{r\theta}}{\partial r} + \frac{1}{r}\frac{\partial \sigma_{\theta\theta}}{\partial \theta} + 2\frac{\tau_{r\theta}}{r} = 0 \tag{6b}$$

$$\frac{\partial \tau_{rz}}{\partial r} + \frac{1}{r}\frac{\partial \tau_{\theta z}}{\partial \theta} + \frac{\tau_{rz}}{r} = 0. \tag{6c}$$

Strain–displacement relation

$$\varepsilon_{rr} = \frac{\partial u_r}{\partial r} \tag{7a}$$

$$\varepsilon_{\theta\theta} = \frac{1}{r}\frac{\partial u_\theta}{\partial \theta} + \frac{u_r}{r} \tag{7b}$$

$$\varepsilon_{zz} = \frac{\partial u_z}{\partial z} \tag{7c}$$

$$\gamma_{r\theta} = \frac{1}{r}\frac{\partial u_r}{\partial \theta} + \frac{\partial u_\theta}{\partial r} - \frac{u_\theta}{r} \tag{7d}$$

$$\gamma_{rz} = \frac{\partial u_z}{\partial r} \tag{7e}$$

$$\gamma_{\theta z} = \frac{1}{r}\frac{\partial u_z}{\partial \theta} \tag{7f}$$

where $u_i$ are the components of the vector of displacement in the cylindrical coordinate system.

Continuity equation

$$\frac{\partial \zeta}{\partial t} - \kappa \nabla^2 p = 0 \tag{8}$$

where $\kappa = k/\mu$ is the permeability in the isotropic plane in which $k$ is the intrinsic permeability in the isotropic plane and $\mu$ is the viscosity of the pore fluid, and $\nabla^2$ is a differential operator expressed by:

$$\nabla^2 = \frac{\partial^2}{\partial r^2} + \frac{1}{r}\frac{\partial}{\partial r} + \frac{1}{r^2}\frac{\partial^2}{\partial \theta^2}. \tag{9}$$

From eqns (8), (6), (3), and (1), we obtained the following fluid variation field equation:

$$\frac{\partial \zeta}{\partial t} - c_T \nabla^2 \zeta = 0 \tag{10}$$

where $c_T$ is a diffusion coefficient in the isotropic plane and may be expressed by:

$$c_T = \frac{\kappa M M_{11}}{M_{11} + \alpha^2 M}. \tag{11}$$

Darcy's law

$$q_r = -\kappa \frac{\partial p}{\partial r} \tag{12a}$$

$$q_\theta = -\kappa \frac{1}{r}\frac{\partial p}{\partial \theta} \tag{12b}$$

$$q_z = 0 \tag{12c}$$

where $q_i$ are the components of the vector of the specific discharge of the pore fluid in the cylindrical coordinate system.

## 3. SOLUTION FOR BOREHOLE PROBLEM

### 3.1. *Problem description*

It is assumed that an infinitely long borehole is drilled perpendicular to the isotropic plane of a transversely isotropic poroelastic formation. The borehole axis is designated as

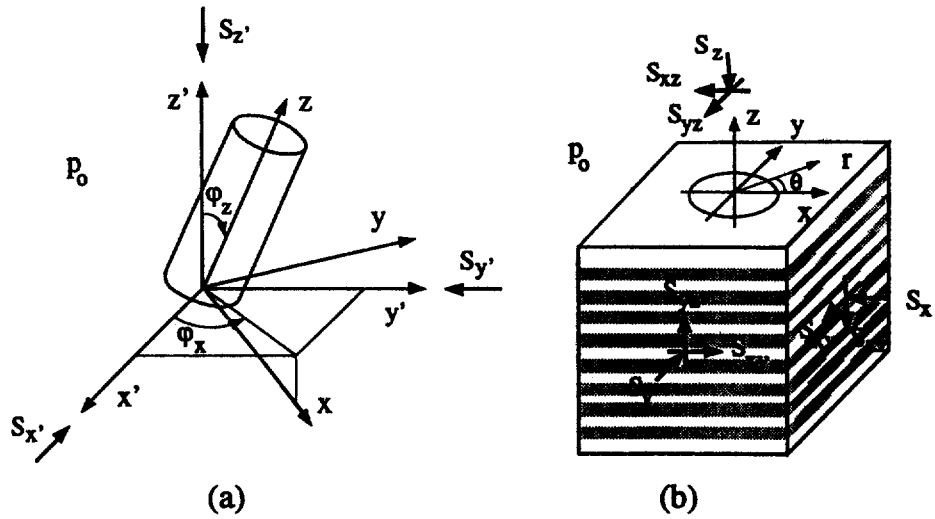


Fig. 1. Inclined borehole in a transversely isotropic material.

the $z$-axis in Fig. 1(a). The principal axes of the far-field stresses are shown as $x'-y'-z'$ with three stress components denoted as $S_{x'}$, $S_{y'}$ and $S_{z'}$. The inclination of the borehole is measured by the angles $\varphi_x$ and $\varphi_z$ as depicted in Fig. 1(a). Figure 1(b) shows the far-field stress components from the vantage-point of the borehole coordinates $x-y-z$. It is noted that there now exist normal and shear stress components denoted by $S_{ij}$.

The boundary conditions of the problem can be imposed in the following: at the far-field, i.e., $r \to \infty$,

$$\sigma_{xx} = -S_x \tag{13a}$$

$$\sigma_{yy} = -S_y \tag{13b}$$

$$\sigma_{zz} = -S_z \tag{13c}$$

$$\tau_{xy} = -S_{xy} \tag{13d}$$

$$\tau_{yz} = -S_{yz} \tag{13e}$$

$$\tau_{xz} = -S_{xz} \tag{13f}$$

$$p = p_0 \tag{13g}$$

where $\sigma_{ii}$ and $\tau_{ij}$ are stress components under the Cartesian coordinate system $xyz$, and $p_0$ is the formation virgin pore pressure; and at the borehole wall, i.e., $r = R$

$$\sigma_{rr} = -p_w \mathrm{H}(t) \tag{14a}$$

$$\tau_{r\theta} = \tau_{rz} = 0 \tag{14b}$$

$$p = p_i \mathrm{H}(t) \tag{14c}$$

in which $p_w$ is the wellbore pressure, $p_i$ is the pore pressure at the borehole wall, and $\mathrm{H}(t)$ is the Heaviside step function. It is noted that $p_i$ is not necessary the same as $p_w$ due to the existence of a filter cake that usually forms in drilling operations.

Because of the linearity of the problem, it can be decomposed into three sub-problems.

*Problem* 1

At the far-field ($r \to \infty$),

$$\sigma_{zz} = -\nu'(S_x + S_y) - (\alpha' - 2\nu'\alpha)p_0 \tag{15a}$$

$$\sigma_{xx} = -S_x \tag{15b}$$

$$\sigma_{yy} = -S_y \tag{15c}$$

$$\tau_{xy} = -S_{xy} \tag{15d}$$

$$p = p_0 \tag{15e}$$

$$\tau_{yz} = \tau_{xz} = 0; \tag{15f}$$

and, at the borehole wall ($r = R$),

$$\sigma_{rr} = -p_w \mathrm{H}(t) \tag{16a}$$

$$\tau_{r\theta} = 0 \tag{16b}$$

$$\tau_{rz} = 0 \tag{16c}$$

$$p = p_i \mathrm{H}(t). \tag{16d}$$

*Problem II*

At the far-field ($r \to \infty$),

$$\sigma_{zz} = -S_z + [\nu'(S_x + S_y) + (\alpha' - 2\nu'\alpha)p_0] \tag{17a}$$

$$\sigma_{xx} = \sigma_{yy} = \tau_{xy} = \tau_{yz} = \tau_{xz} = p = 0; \tag{17b}$$

and, at the borehole wall ($r = R$),

$$\sigma_{rr} = \tau_{r\theta} = \tau_{rz} = p = 0. \tag{18}$$

*Problem III*

At the far-field ($r \to \infty$),

$$\sigma_{xx} = \sigma_{yy} = \sigma_{zz} = \tau_{xy} = p = 0 \tag{19a}$$

$$\tau_{yz} = -S_{yz} \tag{19b}$$

$$\tau_{xz} = -S_{xz}; \tag{19c}$$

and, at the borehole wall ($r = R$),

$$\sigma_{rr} = \tau_{r\theta} = \tau_{rz} = p = 0. \tag{20}$$

3.2. *Correspond elastic case*

Before moving to the poroelastic solution, let us first examine the stresses around the borehole for the corresponding elastic problem. This can be achieved by setting $p = p_0 = p_i = 0$ in the poroelastic problem. When the symmetry axis of the transversely isotropic material coincides with the borehole axis, it can be demonstrated, from the anisotropic elasticity (Amadei, 1983), that the vertical stresses in Problem II and anti-plane shear stresses in Problem III (which are the only non-zero stress components) do not produce any in-plane stress. Therefore, they are totally uncoupled with Problem I. More importantly, Problem II does not disturb the initial stress field at all; and anti-shear stresses in Problem III have no effect on the volumetric strain. This indicates that the original trivial pore pressure fields in Problems II and III are never changed. Therefore, Problems II and III are stand-alone elastic problems, and only Problem I is of a poroelastic nature. In addition, according to the anisotropic elastic borehole solution (Amadei, 1983), the anisotropic elastic solution for stresses of Problem III is exactly the same as the isotropic one.

However, it should be noted that these conditions are no longer valid when the material symmetry axis has an arbitrary inclination. Under this circumstance, the pore pressure may be influenced by an anti-plane shear stress field.

3.3. *Solution for Problem I*

Problem I is a plane strain problem. In elasticity the plane strain solution for stresses in transverse isotropic material is the same as that for the isotropic one, if the plane of symmetry is orthogonal to the material rotational axis of symmetry. While the governing equations of the poroelastic anisotropic case are similar to the isotropic ones, their solutions for stresses are different (Abousleiman *et al.*, 1995; Cui, 1995). The solution for Problem I is then expressed by:

$$\sigma_{rr}^{(\mathrm{I})} = -P_0 + S_0 \cos 2(\theta - \theta_r) + \sigma_{rr}^{(1)} + \sigma_{rr}^{(2)} + \sigma_{rr}^{(3)} \tag{21a}$$

$$\sigma_{\theta\theta}^{(\mathrm{I})} = -P_0 - S_0 \cos 2(\theta - \theta_r) + \sigma_{\theta\theta}^{(1)} + \sigma_{\theta\theta}^{(2)} + \sigma_{\theta\theta}^{(3)} \tag{21b}$$

$$\sigma_{zz}^{(\mathrm{I})} = \nu'[\sigma_{rr}^{(\mathrm{I})} + \sigma_{\theta\theta}^{(\mathrm{I})}] - (\alpha' - 2\nu'\alpha)p^{(\mathrm{I})} \tag{21c}$$

$$\tau_{r\theta}^{(\mathrm{I})} = -S_0 \sin 2(\theta - \theta_r) + \tau_{r\theta}^{(3)} \tag{21d}$$

$$\tau_{rz}^{(\mathrm{I})} = \tau_{\theta z}^{(\mathrm{I})} = 0 \tag{21e}$$

$$p^{(\mathrm{I})} = p_0 + p^{(2)} + p^{(3)} \tag{21f}$$

where

$$P_0 = \frac{S_x + S_y}{2} \tag{22a}$$

$$S_0 = \sqrt{\left(\frac{S_x - S_y}{2}\right)^2 + S_{xy}^2} \tag{22b}$$

$$\theta_r = \frac{1}{2}\tan^{-1}\frac{2S_{xy}}{S_x - S_y}. \tag{22c}$$

Details of the derivations and expressions of $\sigma_{rr}^{(1)}$, $\sigma_{rr}^{(2)}$, $\sigma_{rr}^{(3)}$, $\sigma_{\theta\theta}^{(1)}$, $\sigma_{\theta\theta}^{(2)}$, $\sigma_{\theta\theta}^{(3)}$, $\tau_{r\theta}^{(3)}$, $p^{(2)}$, and $p^{(3)}$ are presented in Appendix A.

3.4. *Solution for Problem II*

As mentioned before, Problem II is purely elastic for the case of material anisotropy concerned within this paper. Its solution for stresses is the same as the one for the corresponding isotropic problem (Cui *et al.*, 1997a), hence,

$$\sigma_{zz}^{(\mathrm{II})} = -S_z + [\nu'(S_x + S_y) + (\alpha' - 2\nu'\alpha)p_0] \tag{23a}$$

$$\sigma_{rr}^{(\mathrm{II})} = \sigma_{\theta\theta}^{(\mathrm{II})} = \tau_{r\theta}^{(\mathrm{II})} = \tau_{rz}^{(\mathrm{II})} = \tau_{\theta z}^{(\mathrm{II})} = p^{(\mathrm{II})} = 0. \tag{23b}$$

In fact, this set of stresses and the pore pressure satisfies all the governing equations, compatibility and boundary conditions; therefore, it forms an admissible poroelastic solution.

Generally speaking, taking off the core material which occupied the borehole geometry originally disturbs initial stress and pore pressure fields around the borehole and results in the redistribution of stresses and pore pressures. Problem II presents the parts of stress and pore pressure fields which are not disturbed through this process. Therefore, its solution must be uniform as the same as its initial state.

3.5. *Solution for Problem III*

This problem is an anti-shear problem. For this special case of transverse isotropy investigated here, the shear deformation is uncoupled with the pore fluid flow. Since the anisotropic elasticity shows that the excavation of the borehole only disturbs the anti-shear stresses, hence the shear deformation, Problem III is also purely elastic. The solution is the same as the elastic one. Under these circumstances, the anisotropy does not affect anti-shear stress fields. (However, the displacements are affected.) Therefore, the solution can be obtained as:

$$\tau_{rz}^{(\mathrm{III})} = -(S_{xz}\cos\theta + S_{yz}\sin\theta)\left[1 - \mathrm{H}(t)\frac{R^2}{r^2}\right] \tag{24a}$$

$$\tau_{\theta z}^{(\mathrm{III})} = (S_{xz}\sin\theta - S_{yz}\cos\theta)\left[1 + \mathrm{H}(t)\frac{R^2}{r^2}\right] \tag{24b}$$

$$\sigma_{rr}^{(\mathrm{III})} = \sigma_{\theta\theta}^{(\mathrm{III})} = \sigma_{zz}^{(\mathrm{III})} = \tau_{r\theta}^{(\mathrm{III})} = p^{(\mathrm{III})} = 0. \tag{24c}$$

3.6. *Final solution*

Finally, the solution for dynamic variables of an inclined borehole in a transversely isotropic poroelastic medium is obtained by superposition; i.e.,

$$\sigma_{rr} = \sigma_{rr}^{(\mathrm{I})} \tag{25a}$$

$$\sigma_{\theta\theta} = \sigma_{\theta\theta}^{(\mathrm{I})} \tag{25b}$$

$$\sigma_{zz} = \sigma_{zz}^{(\mathrm{I})} + \sigma_{zz}^{(\mathrm{II})} \tag{25c}$$

$$\tau_{r\theta} = \tau_{r\theta}^{(\mathrm{I})} \tag{25d}$$

$$\tau_{rz} = \tau_{rz}^{(\mathrm{III})} \tag{25e}$$

$$\tau_{\theta z} = \tau_{\theta z}^{(\mathrm{III})} \tag{25f}$$

$$p = p^{(\mathrm{I})} \tag{25g}$$

in which components that are identically zero are omitted.

## 4. SOLUTION FOR CYLINDER PROBLEMS

4.1. *Problem description*

In this problem, the length of the cylinder is assumed to be much greater than its radius; the isotropic plane of the material symmetry is also normal to the axis of the cylinder (the $z$-axis in Fig. 2); and, the flow in the $z$-direction is not allowed. The boundary

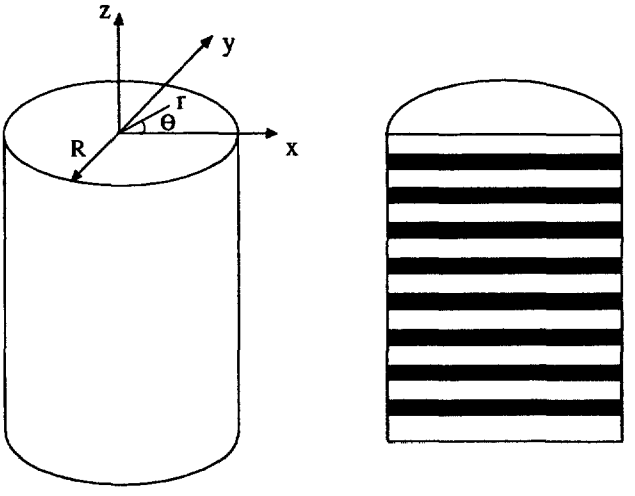


Fig. 2. Schematic of the cylinder.

conditions commonly encountered in the laboratory can be summarized at the cylinder's outer boundary, $r = R$, as:

$$p = p_0(t) \tag{26a}$$

$$q_r = Q(t)/2\pi R \tag{26b}$$

$$\sigma_{rr} = -P_0(t) - S_0 \cos\theta \mathrm{H}(t) \tag{26c}$$

$$\tau_{r\theta} = S_0 \sin 2\theta \mathrm{H}(t) \tag{26d}$$

$$\tau_{rz} = 0. \tag{26e}$$

In addition, a uniform axial strain is imposed which is similar in laboratory tests jargon called a "stroke control test": i.e.,

$$\varepsilon_{zz} = -\varepsilon_0(t). \tag{27}$$

In the above, $p_0$ is a time-dependent pore pressure applied on the cylindrical surface; $Q(t)$ is the total flow discharge across the cylindrical surface per unit length; $P_0$ is the normal pressure applied on the surface and it may be a time-dependent loading; $S_0$ is a constant which represents the amplitude of sinusoidal distributions of normal pressure and shear stress applied on the surface; and $\varepsilon_0$ is the magnitude of the compressive axial strain and may also be time-dependent.

In view of the linearity, the problem can be decomposed into the following modes for which combinations (modes superposition) can simulate many laboratory test configurations:

*Mode* 1

At $r = R$,

$$p = p_0(t) \tag{28a}$$

$$\sigma_{rr} = 0 \tag{28b}$$

$$\tau_{r\theta} = 0 \tag{28c}$$

with the plane strain condition $\varepsilon_{zz} = 0$.

*Mode* 2

At $r = R$,

$$q_r = Q(t)/2\pi R \tag{29a}$$

$$\sigma_{rr} = 0 \tag{29b}$$

$$\tau_{r\theta} = 0 \tag{29c}$$

with the plane strain condition $\varepsilon_{zz} = 0$.

*Mode* 3

At $r = R$,

$$p = 0 \tag{30a}$$

$$\sigma_{rr} = -P_0(t) \tag{30b}$$

$$\tau_{r\theta} = 0 \tag{30c}$$

with the plane strain condition $\varepsilon_{zz} = 0$.

*Mode* 4

At $r = R$,

$$q_r = 0 \tag{31a}$$

$$\sigma_{rr} = -P_0(t) \tag{31b}$$

$$\tau_{r\theta} = 0 \tag{31c}$$

with the plane strain condition $\varepsilon_{zz} = 0$.

*Mode* 5

At $r = R$,

$$p = 0 \tag{32a}$$

$$\sigma_{rr} = -S_0 \cos 2\theta \mathrm{H}(t) \tag{32b}$$

$$\tau_{r\theta} = S_0 \sin 2\theta \mathrm{H}(t) \tag{32c}$$

with the plane strain condition $\varepsilon_{zz} = 0$.

*Mode* 6

At $r = R$,

$$q_r = 0 \tag{33a}$$

$$\sigma_{rr} = -S_0 \cos 2\theta \mathrm{H}(t) \tag{33b}$$

$$\tau_{r\theta} = S_0 \sin 2\theta \mathrm{H}(t) \tag{33c}$$

with the plane strain condition $\varepsilon_{zz} = 0$.

*Mode* 7

At $r = R$,

$$p = 0 \tag{34a}$$

$$\sigma_{rr} = 0 \tag{34b}$$

$$\tau_{r\theta} = 0 \tag{34c}$$

$$\tau_{rz} = 0 \tag{34d}$$

with a generalized plane strain condition $\varepsilon_{zz} = -\varepsilon_0$.

*Mode* 8

At $r = R$,

$$q_r = 0 \tag{35a}$$

$$\sigma_{rr} = 0 \tag{35b}$$

$$\tau_{r\theta} = 0 \tag{35c}$$

$$\tau_{rz} = 0 \tag{35d}$$

with a generalized plane strain condition $\varepsilon_{zz} = -\varepsilon_0$.

Except for Modes 5 and 6, which are asymmetric, all other modes are axisymmetric. Modes 5 and 6 are solved below first. Then, the general solution for the axisymmetric

cylinder problem is derived. Hence, all axisymmetric modes are solved according to the corresponding boundary conditions.

4.2. *Solution for asymmetric problem*

Modes 5 and 6 are asymmetric problems. Their corresponding elastic solution can be obtained as:

$$\sigma_{rr} = -S_0 \cos 2\theta \mathrm{H}(t) \tag{36a}$$

$$\sigma_{\theta\theta} = S_0 \cos 2\theta \mathrm{H}(t) \tag{36b}$$

$$\tau_{r\theta} = S_0 \sin 2\theta \mathrm{H}(t) \tag{36c}$$

$$\sigma_{zz} = 0. \tag{36d}$$

It is noted that according to the formula (5), the stress field expressed by (36) does not result in any variation of the pore pressure at the undrained state, and the flow boundary conditions for Modes 5 and 6 are trivial. Hence, the pore pressure distribution in the cylinder for Modes 5 and 6 must also be trivial since there is no disturbance subjected to the stress field (36). In other words, Modes 5 and 6 are purely elastic. Therefore, the solution for Modes 5 and 6 are exactly the same as their elastic counterparts and expressed by:

$$\sigma_{rr} = -S_0 \cos 2\theta \mathrm{H}(t) \tag{37a}$$

$$\sigma_{\theta\theta} = S_0 \cos 2\theta \mathrm{H}(t) \tag{37b}$$

$$\tau_{r\theta} = S_0 \sin 2\theta \mathrm{H}(t) \tag{37c}$$

$$\sigma_{zz} = 0 \tag{37d}$$

$$p = 0. \tag{37e}$$

4.3. *Solution for axisymmetric problem*

For an axisymmetric cylinder problem, such as all other modes except for Modes 5 and 6, the axisymmetry leads to:

$$u_\theta = 0 \tag{38a}$$

$$q_\theta = 0 \tag{38b}$$

$$\tau_{r\theta} = \tau_{rz} = \tau_{\theta z} = 0. \tag{38c}$$

Except that $u_z$ is a function of $r$, $z$, and $t$, all other variables, such as $\sigma_{rr}$, $\sigma_{\theta\theta}$, $\sigma_{zz}$, $p$, $q_r$ and $u_r$, are functions of the radial distance $r$ and time $t$ only. The general solution for an axisymmetric cylinder problem can be derived analytically in the Laplace transform domain. The solution in the time domain is obtained via the inverse of the Laplace transform through a numerical technique (Stehfest, 1970).

Because of axisymmetry, the diffusion eqn (10) can be written as:

$$\frac{\partial \zeta}{\partial t} - c_T \left( \frac{\partial^2 \zeta}{\partial r^2} + \frac{1}{r} \frac{\partial \zeta}{\partial r} \right) = 0. \tag{39}$$

Applying the Laplace transform to eqn (39) yields:

$$\frac{\mathrm{d}^2 \tilde{\zeta}}{\mathrm{d}r^2} + \frac{1}{r} \frac{\mathrm{d}\tilde{\zeta}}{\mathrm{d}r} - \frac{s}{c_T} \tilde{\zeta} = 0 \tag{40}$$

where $\tilde{}$ denotes the Laplace transform and $s$ is the Laplace transform variable. Setting $\xi = r\sqrt{s/c_T}$, it is obtained that:

$$\frac{\alpha M}{M_{11}+\alpha^2 M}\tilde{\zeta} = A_1 \mathrm{I}_0(\xi). \tag{41}$$

Applying the solution for the fluid content variation $\tilde{\zeta}$ and using constitutive relations (1) and (3), the strain–displacement relation (7), and Darcy's law (12), the general solution for the axisymmetric cylinder problem (associated with Modes 1–4, 7, or 8) is derived as:

$$\tilde{u}_r = \frac{A_1}{\sqrt{s/c_T}}\mathrm{I}_1(\xi) + A_2 r \tag{42a}$$

$$\tilde{p} = \frac{M_{11}}{\alpha} A_1 \mathrm{I}_0(\xi) - 2\alpha M A_2 - \alpha' M \tilde{\varepsilon}_{zz} \tag{42b}$$

$$\tilde{q}_r = -\kappa \sqrt{\frac{s}{c_T}} \frac{M_{11}}{\alpha} A_1 \mathrm{I}_1(\xi) \tag{42c}$$

$$\frac{\tilde{\sigma}_{rr}}{2G} = -A_1 \frac{\mathrm{I}_1(\xi)}{\xi} + \frac{M_{11}+M_{12}+2\alpha^2 M}{2G} A_2 + \frac{M_{13}+\alpha\alpha' M}{2G}\tilde{\varepsilon}_{zz} \tag{42d}$$

$$\frac{\tilde{\sigma}_{\theta\theta}}{2G} = -A_1 \left(\mathrm{I}_0(\xi) - \frac{\mathrm{I}_1(\xi)}{\xi}\right) + \frac{M_{11}+M_{12}+2\alpha^2 M}{2G} A_2 + \frac{M_{13}+\alpha\alpha' M}{2G}\tilde{\varepsilon}_{zz} \tag{42e}$$

$$\tilde{\sigma}_{zz} = -\left(\frac{\alpha'}{\alpha} M_{11} - M_{13}\right) A_1 \mathrm{I}_0(\xi) + 2(M_{13}+\alpha\alpha' M) A_2 + (M_{33}+\alpha'^2 M)\tilde{\varepsilon}_{zz}. \tag{42f}$$

In the above, $A_1$ and $A_2$ are arbitrary functions of the Laplace transform variable $s$; and $\mathrm{I}_n$ is the modified Bessel function of the first kind of order $n$. For individual problems, $A_1$ and $A_2$ can be determined from corresponding loading and boundary conditions. For Modes 1–4, 7, and 8, $A_1$ and $A_2$ are obtained below:

*Mode* 1

$$\tilde{\varepsilon}_{zz} = 0 \tag{43a}$$

$$A_1 = \tilde{p}_0 \frac{M_{11}+M_{12}+2\alpha^2 M}{2G} \frac{\beta}{C_1 \mathrm{I}_1(\beta)} \tag{43b}$$

$$A_2 = \frac{\tilde{p}_0}{C_1} \tag{43c}$$

where $\beta = R\sqrt{s/c_T}$, and $C_1$ is expressed by:

$$C_1 = \frac{M_{11}+M_{12}+2\alpha^2 M}{2G} \frac{M_{11}}{\alpha} \frac{\beta \mathrm{I}_0(\beta)}{\mathrm{I}_1(\beta)} - 2\alpha M. \tag{44}$$

*Mode* 2

$$\tilde{\varepsilon}_{zz} = 0 \tag{45a}$$

$$A_1 = -\frac{\tilde{Q}}{2\pi\beta} \frac{\alpha}{\kappa M_{11} \mathrm{I}_1(\beta)} \tag{45b}$$

$$A_2 = -\frac{\tilde{Q}}{2\pi\beta^2} \frac{2\alpha G}{\kappa M_{11}(M_{11}+M_{12}+2\alpha^2 M)}. \tag{45c}$$

*Mode* 3

$$\tilde{\varepsilon}_{zz} = 0 \tag{46a}$$

$$A_1 = -\frac{\tilde{P}_0}{GC_3}\frac{\alpha^2 M}{M_{11}\mathrm{I}_0(\beta)} \tag{46b}$$

$$A_2 = -\frac{\tilde{P}_0}{2GC_3} \tag{46c}$$

where $C_3$ is expressed by:

$$C_3 = \frac{M_{11}+M_{12}+2\alpha^2 M}{2G} - \frac{2\alpha^2 M}{M_{11}}\frac{\mathrm{I}_1(\beta)}{\beta \mathrm{I}_0(\beta)}. \tag{47}$$

*Mode* 4

$$\tilde{\varepsilon}_{zz} = 0 \tag{48a}$$

$$A_1 = 0 \tag{48b}$$

$$A_2 = -\frac{\tilde{P}_0}{M_{11}+M_{12}+2\alpha^2 M}. \tag{48c}$$

*Mode* 7

$$\tilde{\varepsilon}_{zz} = -\tilde{\varepsilon}_0 \tag{49a}$$

$$A_1 = -\tilde{\varepsilon}_0 \frac{1}{M_{11}\mathrm{I}_0(\beta)}\left(\alpha\alpha' M + 2\alpha^2 M\frac{C_7}{C_3}\right) \tag{49b}$$

$$A_2 = -\tilde{\varepsilon}_0 \frac{C_7}{C_3} \tag{49c}$$

where $C_3$ is given by eqn (47) and $C_7$ is expressed by:

$$C_7 = \frac{\alpha\alpha' M}{M_{11}}\frac{\mathrm{I}_1(\beta)}{\beta \mathrm{I}_0(\beta)} - \frac{M_{13}+\alpha\alpha' M}{2G}. \tag{50}$$

*Mode* 8

$$\tilde{\varepsilon}_{zz} = -\tilde{\varepsilon}_0 \tag{51a}$$

$$A_1 = 0 \tag{51b}$$

$$A_2 = \tilde{\varepsilon}_0 \frac{M_{13}+\alpha\alpha' M}{M_{11}+M_{12}+2\alpha^2 M}. \tag{51c}$$

It should be noted that $A_1$ in Modes 4 and 8 is zero; hence, no flow takes place in the cylinder. In fact, for Modes 4 and 8 the pore pressure is identical everywhere, and the boundary surface is impermeable (jacketed test). Therefore, the pore fluid is not allowed to flow in the cylinder; and the modes represent the undrained state; i.e., solutions for Modes 4 and 8 are what we call the "undrained solutions".

## 5. NUMERICAL EXAMPLES

### 5.1. *Material anisotropy*

For transversely isotropic materials with micro-homogeneous and micro-isotropic solid skeletons, the poroelastic constants (Biot's effective stress parameter) $\alpha$ and $\alpha'$ can be expressed in terms of $M_{ij}$ and the bulk modulus of the solid grains, $K_s$ (Cheng, 1997):

$$\alpha = 1 - \frac{M_{11} + M_{12} + M_{13}}{3K_s} \tag{52a}$$

$$\alpha' = 1 - \frac{2M_{13} + M_{33}}{3K_s}. \tag{52b}$$

Therefore, Young's moduli and Poisson's ratios (which lead to all necessary $M_{ij}$), $M$, and $K_s$ are enough to define the transversely isotropic poroelastic constitutive relations. As an example, it is assumed that $E = 20.6$ GPa, $v = 0.189$, $M = 15.8$ GPa, $K_s = 48.2$ GPa, and $\kappa = \kappa' = 8.64 \times 10^{-6}$ m$^2$/MPa day (Cui *et al.*, 1996b). For given anisotropic ratios of $n_E = E/E'$ and $n_v = v/v'$, $E'$ and $v'$ can be determined; hence, a transversely isotropic material is defined. Different ratios of $n_E$ and $n_v$ define different degrees of anisotropy, and for $n_E = n_v = 1$ the material is isotropic. In the following examples, various ratios of $E/E'$ and $v/v'$ were chosen to demonstrate the effect of anisotropy.

### 5.2. *Inclined borehole*

The far-field *in situ* stress and formation pore pressure gradients adopted for the analysis are the following (Woodland, 1990): $S_{x'} = 29$ MPa/km, $S_{y'} = 20$ MPa/km, $S_{z'} = 25$ MPa/km, and $p_0 = 9.8$ MPa/km. The radius of the borehole was assumed to be $R = 0.1$ m. The deviation of the borehole was defined by $\varphi_x = 30°$ and $\varphi_z = 60°$; and the depth of the formation was assumed to be 1000 m. For the sake of convenience, only the case of an excavation was analyzed; i.e., the well pressure was assumed to be zero.

Numerical results are presented in Figs 3–7. In all the figures, the effective stress indicates Terzaghi's effective stress $(\sigma_{ij} + p\delta_{ij})$; and the negative values of stresses are presented so that the results imply the rock mechanics sign convention for stresses (i.e., positive for compression). All calculated pore pressures and stresses are presented as varying with $r/R$ along $\theta = 90°$.

Figure 3 presents the pore pressure profiles with $n_v = 0.5$, 1, 2 for fixed $n_E = 1$ at different times. It is observed that the material anisotropy influences the pore pressure only at small times ($t = 0.001$ day). For a long time duration ($t = 1$ day), all pore pressure distributions for different $n_v$ are identical; indicating that Poisson's ratios anisotropy does not affect pore pressure at large times.

In Fig. 4 the effective radial stress distribution shows similar results of the anisotropy effect as for the pore pressure. The stress for $n_v = 0.5$ is influenced much more by the anisotropy than for $n_v = 2$. However, unlike the case for the pressure, the anisotropy effect on the stress still exists at large times. It seems that the anisotropy effect on the effective radial stress becomes more significant at places far away from the borehole wall as time progresses.

Figures 5 and 6 describe, respectively, the effective tangential and axial stresses around the borehole. It can be seen from these figures that at small time ($t = 0.001$ day) for different ratios of $n_v$ magnitudes of stresses around the borehole are quite different, but they are close at the places away from the borehole. When time duration becomes longer ($t = 1$ day), the anisotropy effect on stresses is transmitted to the places away from the borehole. It should also be noted that the material anisotropy effect is significant on effective tangential and axial stresses compared to the pore pressure and the radial stress; thus affecting wellbore stability analyses.

For the cases of varied $n_E$ with fixed $n_v = 1$, analyses showed that material anisotropy effects on the pore pressure and all effective stresses are qualitatively similar to the previous

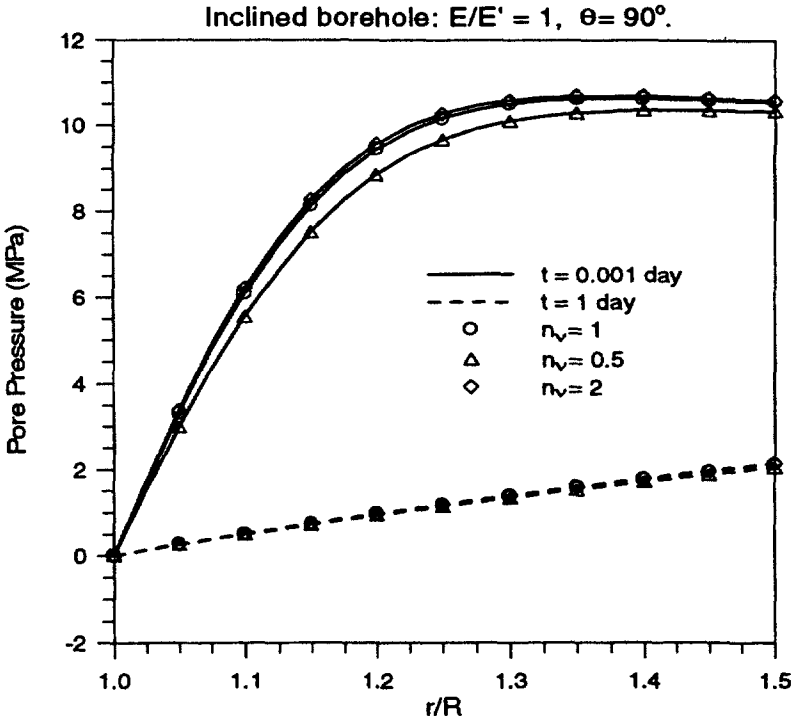


Fig. 3. For $E/E' = 1$ and along the direction of $\theta = 90°$, pore pressure ($p$) near the borehole varying with $r/R$.

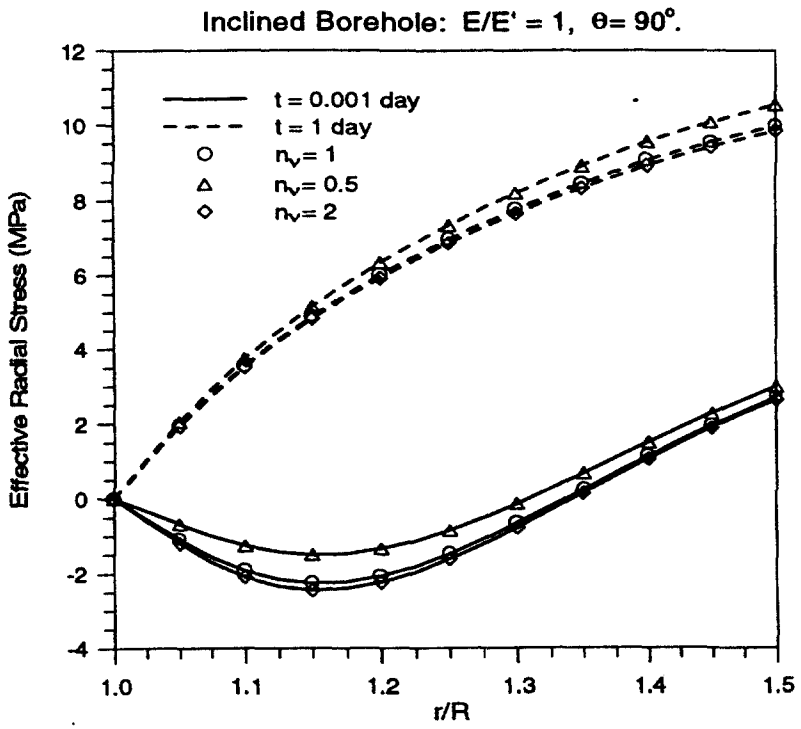


Fig. 4. For $E/E' = 1$ and along the direction of $\theta = 90°$, effective radial stress ($-\sigma'_{rr}$) near the borehole varyuing with $r/R$.

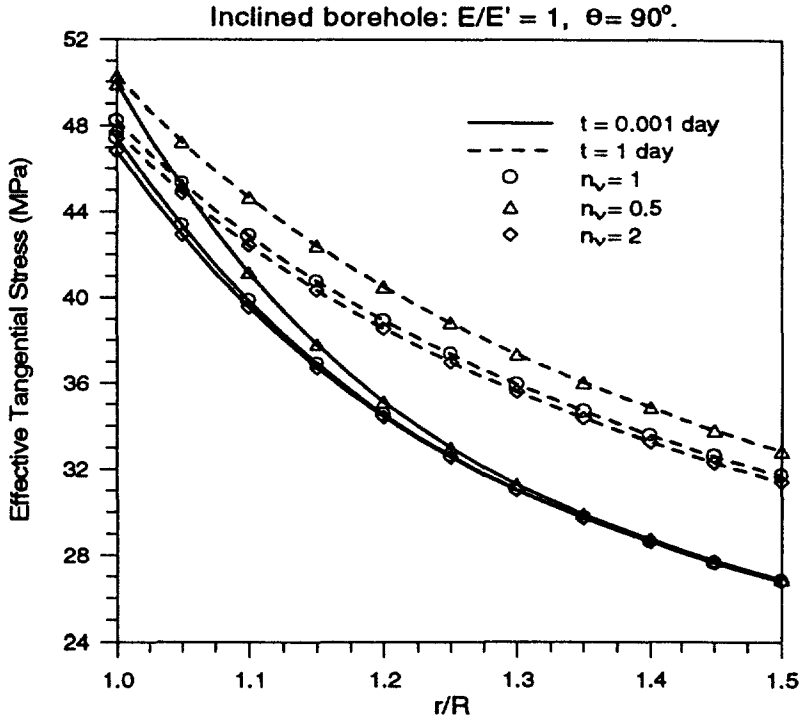


Fig. 5. For $E/E' = 1$ and along the direction of $\theta = 90°$, effective tangential stress $(-\sigma'_{\theta\theta})$ near the borehole varying with $r/R$.

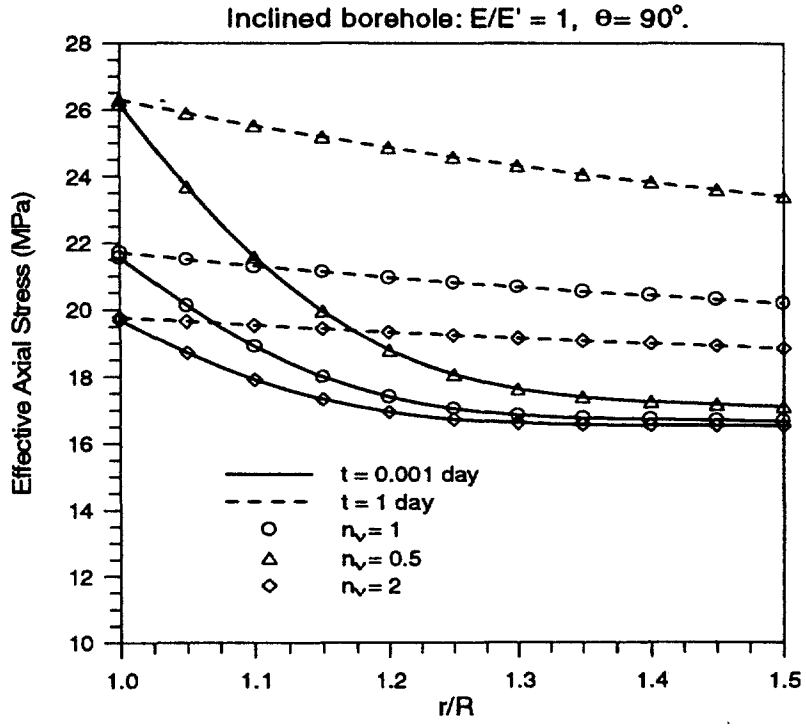


Fig. 6. For $E/E' = 1$ and along the direction of $\theta = 90°$, effective axial stress $(-\sigma'_{zz})$ near the borehole varying with $r/R$.

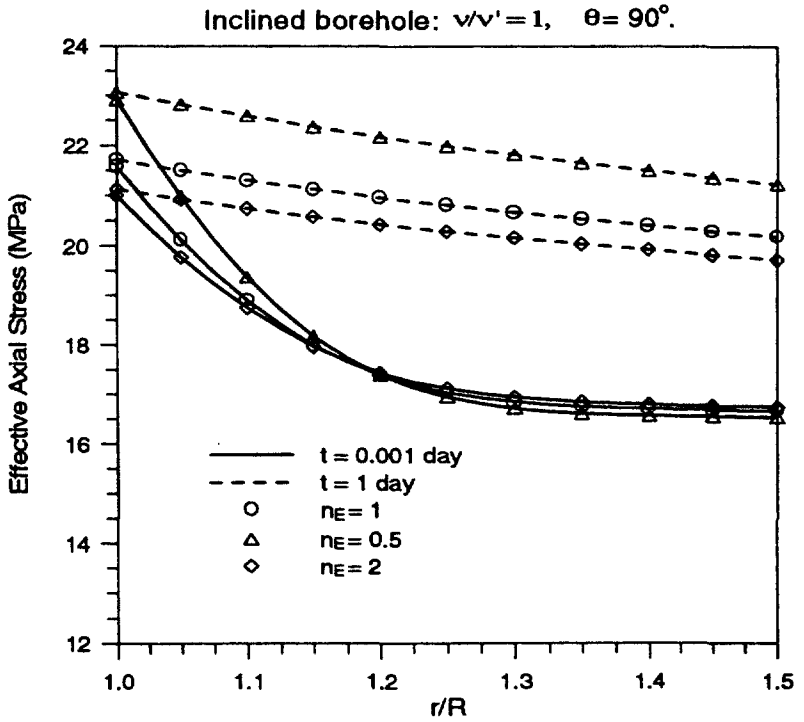


Fig. 7. For $v/v' = 1$ and along the direction of $\theta = 90°$, effective axial stress $(-\sigma'_{zz})$ near the borehole varying with $r/R$.

cases of varied $n_v$. However, considerable effects of anisotropy are exhibited in the calculation of the effective axial stresses as shown in Fig. 7. Similar to the cases of varied $n_v$, the material anisotropy related to the difference between $E$ and $E'$ influences the effective axial stress considerably. Notice that material anisotropy would have a combination of these two ratios, and the corresponding analysis should be conducted.

5.3. *Cylinder*

The radius of the cylinder was set to 0.1 m. It was assumed that a linearly time-dependent compressive axial strain rate ("stroke rate") of $10^{-8}$ 1/s had been applied; i.e., $\varepsilon_{zz} = -10^{-8}\, t$ with a free stress at the cylindrical boundary, $\sigma_{rr} = \tau_{r\theta} = \tau_{rz} = p = 0$. These conditions results in a uniaxial problem for an elastic medium; however, a poroelastic cylinder behave pseudo-three-dimensional.

Figure 8 presents the pore pressure at the center of the cylinder as a function of time for the cases of $n_v = 0.5$, 1, 2 with $n_E = 1$. It is observed that the pore pressure increases from the initial (trivial) level once the axial strain is applied. After a certain time duration, it keeps a constant level as time increases, since the pore pressure field in the cylinder becomes steady. The magnitude of the pore pressure changes significantly with varied ratio of $n_v$. The greater the $n_v$, the higher the pore pressure. In Fig. 9 the pore pressure at the center of the cylinder is plotted for the cases of $n_E = 0.5$, 1, 2 with $n_v = 1$. Similar phenomena to the previous ones are observed.

Figures 10 and 11 show the tangential stresses at the boundary surface ($r = R$) for the cases of fixed $n_E$ and $n_v$, respectively. The material anisotropy and time effects on the tangential stress are qualitatively similar to those on the pore pressure at the center. It is known that for a non-porous elastic cylinder under the same boundary conditions the problem is uniaxial and the tangential stress is trivial. However, for the poroelastic problem a tensile tangential stress is developed as time increases. This suggests that the saturated cylinder may be fracturing due to a compressive axial strain.

The total axial stress at the center varying with time for the cases of $n_E = 0.5$, 1, 2 with $n_v = 1$ is displayed in Fig. 12. In the figure, the negative values of the stress (i.e., positive

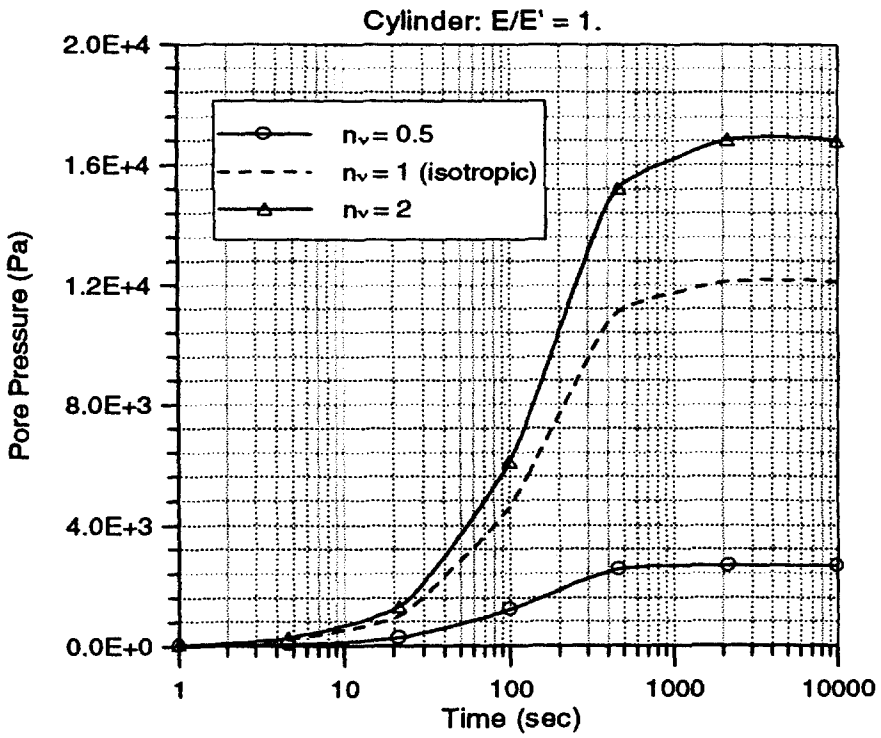


Fig. 8. For $E/E' = 1$, pore presdsure ($p$) at $r = 0$ in the cylinder varyuing with time.

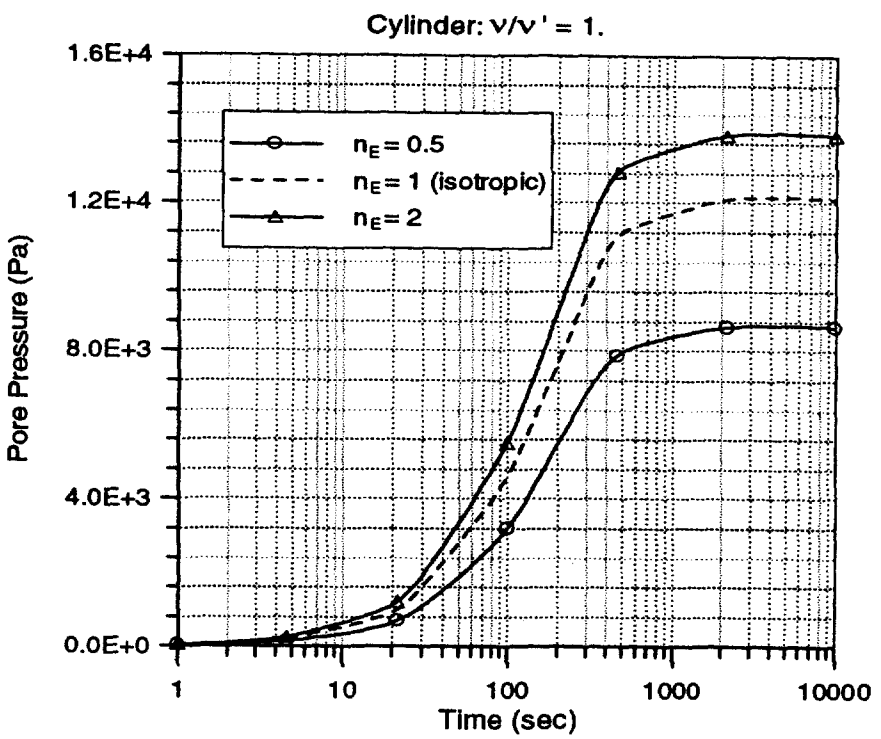


Fig. 9. For $v/v' = 1$, pre pressure ($p$) at $r = 0$ in the cylinder varying with time.

indicates a compressive stress) varying with time are plotted. The axial stress is almost linearly dependent of time. Material anisotropy effect on the stress is considerable; the magnitude of the stress increases as the ratio $n_E$ decreases. It is noted that the magnitude

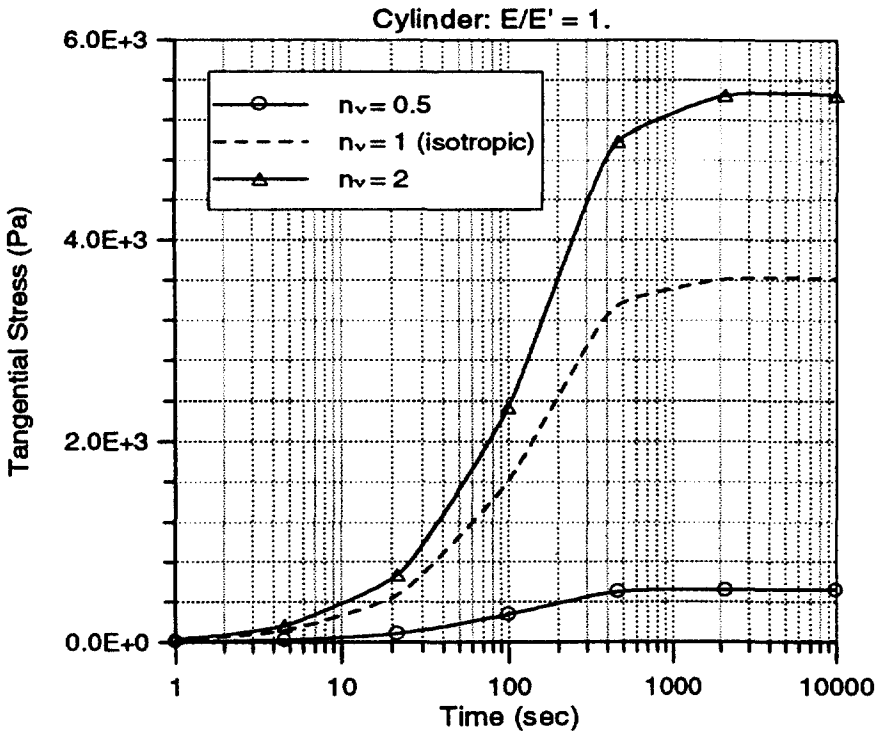


Fig. 10. For $E/E' = 1$, tangential stress ($\sigma_{\theta\theta}$) at $r = R$ in the cylinder varyuing with time.

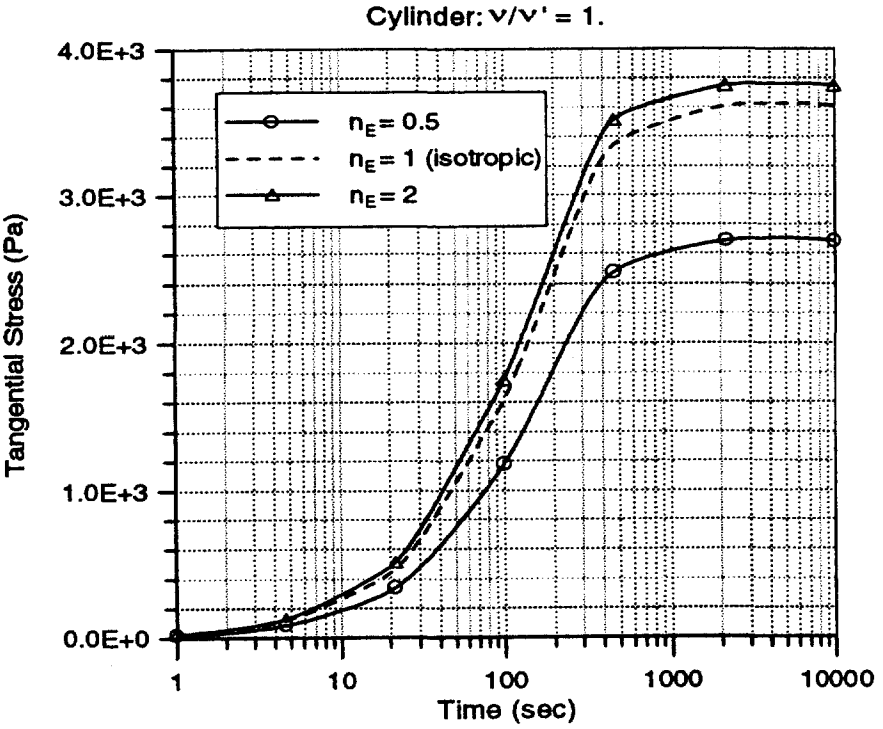


Fig. 11. For $\nu/\nu' = 1$, tangential stress ($\sigma_{\theta\theta}$) at $r = R$ in the cylinder varying with time.

of the axial stress is much greater than the ones of all other dynamic variables. Considering that the slow axial strain rate and the free stress boundary conditions were applied, these results are expected. Although the results are not presented, it is of interest to point out

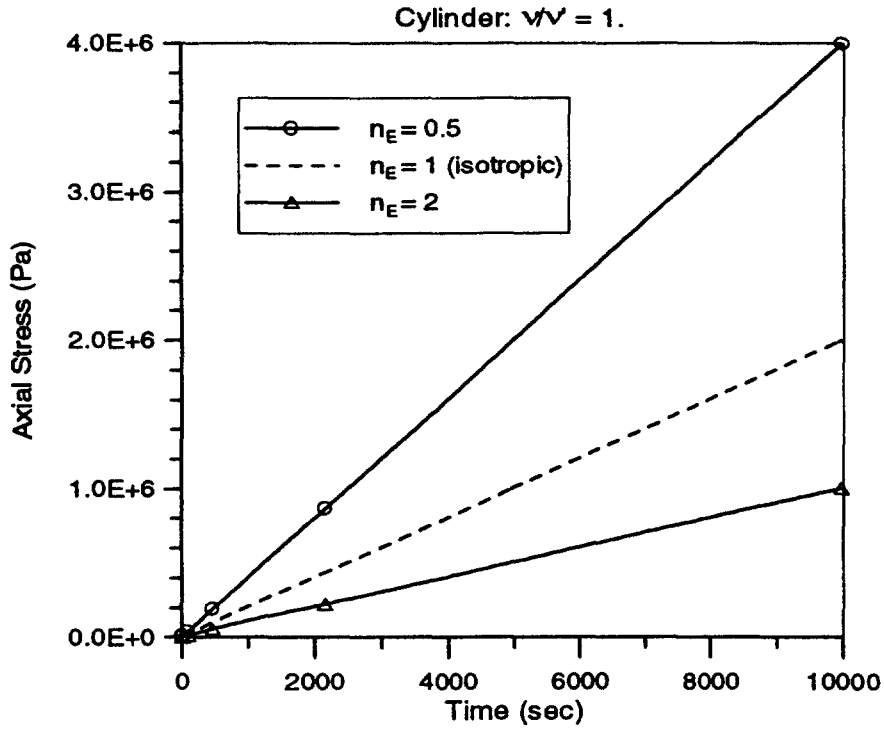


Fig. 12. For $v/v' = 1$, axial stress $(-\sigma_{zz})$ at $r = 0$ in the cylinder varying with time.

that the effect of variation of $n_v$ on the axial stress, on the other hand, is negligible for $n_E = 1$. This indicates that the difference between two Poisson's ratios may not be a major factor as material anisotropy to influence the axial stress.

In contrast with the axial stress, the radial displacement at the boundary surface is sensitive to the variation of $n_v$, but insignificantly influenced by the change of $n_E$. The displacement varying with time for cases of $n_v = 0.5$, 1, 2 with $n_E = 1$ is presented in Fig. 13. It is observed that the displacement is also almost linearly dependent of time and a greater ratio $n_v$ leads to a larger displacement.

Finally, unlike the elastic problem, with coupled pore fluid effect the cylinder problem under Mode 7 is not uniform any more. A non-trivial pore pressure field results from the compaction of the cylinder; and this field is not uniform because of the zero pore pressure condition enforced at the boundary. Hence, the deformation in the axial direction is resisted by the pore fluid and the resistance is also spatially-dependent. This is basically why the poroelastic problem is pseudo-three-dimensional. The radial and tangential stresses are thus generated in the poroelastic problem. Figures 14 and 15 present the variations of the axial stress and pore pressure along the radial direction at $t = 3$ min and $t = 30$ min. Non-uniform stress and pore pressure fields are observed in the figures. Inhomogeneity of stress and pore pressure fields is affected by the anisotropy of Poisson's ratios. If the strain rate is very small and the sample permeability is large, the poroelastic effect may not be significant; hence, the anisotropy effect on the axial stress may not be very pronounced, and could be equivalent to the corresponding elastic cases. However, if the loading rate is considerable and the permeability is small enough (Abousleiman *et al.*, 1996b), the pore pressure generated will be significant and may be comparable to the axial stress.

## 6. CONCLUSIONS AND DISCUSSIONS

For this special form of anisotropy in which the isotropic plane of the transversely isotropic material is perpendicular to the borehole axis and cylinder axis, the poroelastic solutions for inclined boreholes and cylinders have been derived. The borehole solution

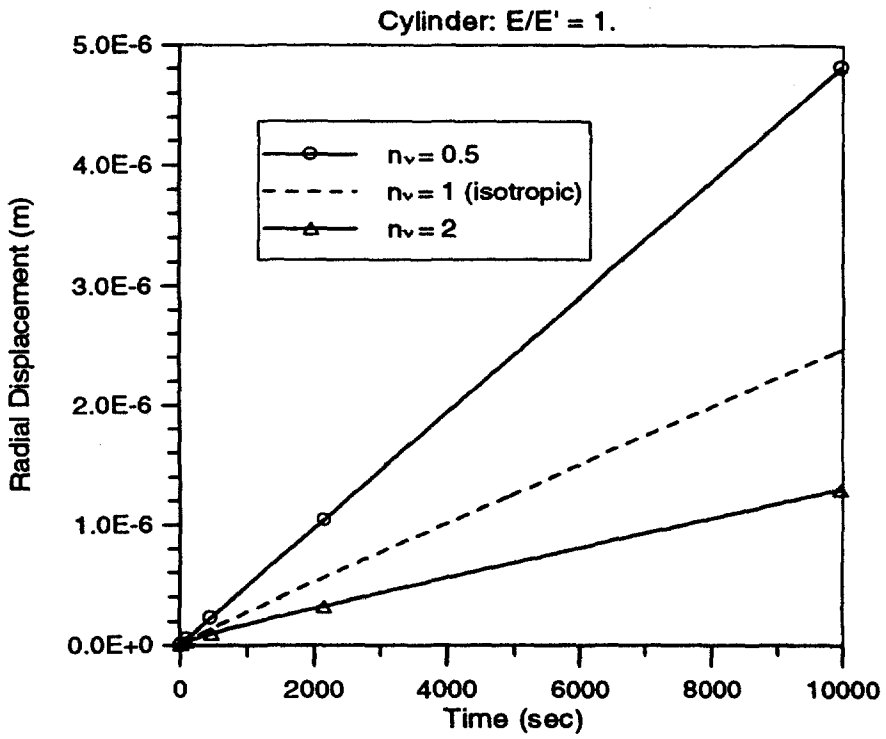


Fig. 13. For $E/E' = 1$, radial displacement ($u_r$) at $r = R$ in the cylinder varyuing with time.

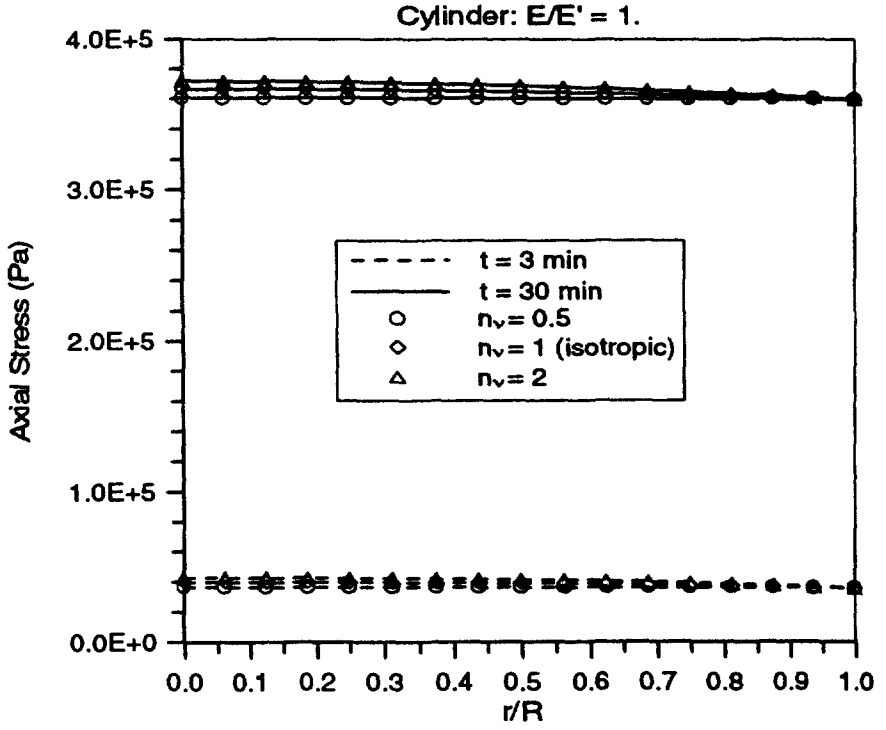


Fig. 14. For $E/E' = 1$, axial stress ($-\sigma_{zz}$) in the cylinder varying with $r/R$ at different times.

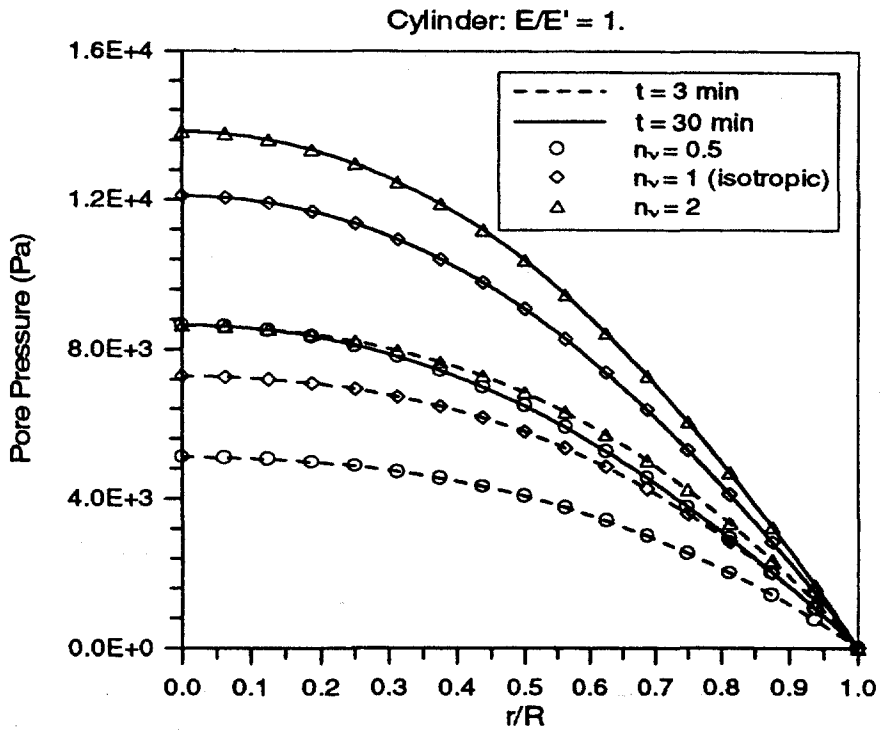


Fig. 15. For $E/E' = 1$, pore presdsure ($p$) in the cylinder varying with $r/R$ at different times.

may be applied to limited cases in practice. However, the cylinder solution can be applied to measurements of poroelastic properties of transversely isotropic materials, as well as the strain recovery method for *in situ* stress determinations in transversely isotropic formations.

The analyses of an inclined borehole show that effective stresses and pore pressure around the borehole are influenced considerably by the material anisotropy, especially when the Poisson's ratio in the isotropic plane is smaller than the Poisson's ratio related to the $z$-direction. Particularly, the material anisotropy effect on the effective tangential and axial stresses is significant. Therefore, it is expected that the material anisotropy influences the borehole stability significantly, while the corresponding elastic solution predicts no anisotropy effect on the fracturing at all.

A cylinder subjected to an axial strain was also analyzed. The results indicate that, unlike the elastic cases, the poroelastic cylinder is a pseudo-three-dimensional problem. A pore pressure field, as well as tangential and radial stress fields, are generated due to the compaction of the cylinder. The material anisotropy effect on these fields is significant. The analyses also show that if the axial strain rate is very small, the magnitudes of generated pore pressure and in-plane stresses may not be significant compared to the axial stress. However, for the materials with lower tensile strength, such as soils and rocks, the induced tensile stress may be high enough to fracture the specimen.

*Acknowledgements*—The work is supported by a National Science Foundation grant to the Rock Mechanics Research Center, the Oklahoma Center for the Advancement of Science and Technology, and the O.U. Rock Mechanics Consortium. Discussions with Prof. A. H.-D. Cheng of University of Delaware and Prof. J.-C. Roegiers of University of Oklahoma were beneficial to the writing of this paper.

## REFERENCES

Abousleiman, Y., Cui, L., Cheng, A. H.-D. and Roegiers, J.-C. (1995) Poroelastic solution of an inclined borehole in a transversely isotropic medium. *Proceedings of the 35th U.S. Symposium on Rock Mechanics*, eds J. J. K. Daemen and R. A. Schultz.

Abousleiman, Y., Cheng, A. H.-D., Cui, L., Detournay, E. and Roegiers, J.-C. (1996a) Mandel's problem revisited. *Géotechnique* **46**(2), 187–195.

Abousleiman, Y., Cheng, A. H.-D., Jiang, C. and Roegiers, J.-C. (1996b) Poroviscoelastic analysis of borehole and cylinder problems. *Acta Mechanica* **119,** 119–219.
Amadei, B. (1983) *Rock Anisotropy and the Theory of Stress Measurements*. Springer-Verlag.
Biot, M. A. (1955) Theory of elasticity and consolidation of a porous anisotropic solid. *Journal of Applied Physics* **26,** 182–185.
Biot, M. A. and Willis, D. G. (1957) The elastic coefficients of the theory of consolidation. *Journal of Applied Mechanics* **24,** 594–601.
Cheng, A. H.-D. (1997) Material coefficient of anisotropic poroelasticity. *Int. J. Rock Mech. Min. Sci.* **34,** 199–205.
Cui, L. (1995) Poroelasticity with application to rock mechanics. Ph.D. dissertation, University of Delaware.
Cui, L., Cheng, A. H.-D. and Abousleiman, Y. (1997a) Poroelastic solution for an inclined borehole. *Journal of Applied Mechanics, ASME* **64,** 32–38.
Cui, L., Abousleiman, Y., Cheng, A. H.-D. and Roegiers, J.-C. (1996a) Anisotropic effect on one-dimensional consolidation. *Engineering Mechanics, Vol.* 1, *Proceedings of the* 11*th Engineering Mechanics Conference, ASCE*, ed. Y. K. Lin and T. C. Su, pp. 471–474.
Cui, L., Abousleiman, Y., Cheng, A. H.-D., Kaliakin, V. N. and Roegiers, J.-C. (1996b) Finite element analysis of anisotropic poroelasticity: a generalized Mandel's problem and an inclined borehole problem. *Int. J. Numer. Anal. Methods Geomech.* **20,** 381–401.
Cui, L., Kaliakin, V. N., Abousleiman, Y. and Cheng, A. H.-D. (1997b) Finite element formulation and application of poroelastic generalized plane strain problems. *Int. J. Rock Mech. Min. Sci.* **34**(6), 953–962.
Detournay, E. and Cheng, A. H.-D. (1988) Poroelastic response of a borehole in a non-hydrostatic stress field. *Int. J. Rock Mech. Min. Sci. Geomech. and Abstr.* **25,** 171–182.
Rice, J. R. and Clearly, M. P. (1976) Some basic stress diffusion solutions for fluid-saturated elastic porous media with compressible constituents. *Reviews of Geophysics and Space Physics* **14**(4), 227–241.
Stehfest, H. (1970) Numerical inversion of Laplace transforms. *Comm. ACM.* **13,** 47–49 and 624.
Thompson, M. and Willis, J. R. (1991) A reformulation of the equations of anisotropic poroelasticity. *Journal of Applied Mechanics, ASME* **58,** 612–616.
Woodland, D. C. (1990) Borehole instability in the western Canadian overthrust belt. *SPE Drill. Eng.* **5,** 27–33.

## APPENDIX

In the solution for Problem I expressed by eqn (21), superscript "$i$" on the right-hand side indicates the corresponding solution for the $i$th mode which was described in Detournay and Cheng (1988). Actually, Modes 1, 2, and 3 are three different special plane strain borehole problems. In all three modes, the boundary conditions at infinity ($r \to \infty$) are set as:

$$\sigma_{rr}^{(i)} = \tau_{r\theta}^{(i)} = p^{(i)} = 0. \tag{53}$$

However, each mode has different boundary conditions at the borehole wall. More specifically:

*Mode* 1

At $r = R$,

$$\sigma_{rr}^{(1)} = (P_0 - p_w)\mathrm{H}(t); \quad \tau_{r\theta}^{(1)} = p^{(1)} = 0. \tag{54}$$

*Mode* 2

At $r = R$,

$$\sigma_{rr}^{(2)} = \tau_{r\theta}^{(2)} = 0; \quad p^{(2)} = -(p_0 - p_i)\mathrm{H}(t). \tag{55}$$

*Mode* 3

At $r = R$,

$$\sigma_{rr}^{(3)} = -S_0 \cos 2(\theta - \theta_r)\mathrm{H}(t); \quad \tau_{r\theta}^{(3)} = S_0 \sin 2(\theta - \theta_r)\mathrm{H}(t); \quad p^{(3)} = 0. \tag{56}$$

Similar to the isotropic problem, the first two modes are axisymmetric problems. The diffusion of pore pressure can thus be uncoupled from the solid deformation; and is governed by:

$$\frac{\partial p}{\partial t} - c_T\left(\frac{\partial^2 p}{\partial r^2} + \frac{1}{r}\frac{\partial p}{\partial r}\right) = 0. \tag{57}$$

It can be derived that the axisymmetry also leads to:

$$u_r = \frac{A}{r} + \frac{\alpha}{M_{11}}\frac{1}{r}\int_a^r rp\,\mathrm{d}r \tag{58}$$

where $A$ is an integration constant. In the above, all variables are finite and $\varepsilon = 0$ at infinity is implied. Therefore, the stresses can be expressed by:

$$\sigma_r = -2G\frac{A}{r^2} - \alpha\left(1-\frac{M_{12}}{M_{11}}\right)\frac{1}{r^2}\int_a^r rp\,dr \tag{59a}$$

$$\sigma_\theta = 2G\frac{A}{r^2} + \alpha\left(1-\frac{M_{12}}{M_{11}}\right)\frac{1}{r^2}\int_a^r rp\,dr - \alpha\left(1-\frac{M_{12}}{M_{11}}\right)p. \tag{59b}$$

Similar to the case of Problem III of the cylinder, Mode 1 can be proven to be purely elastic since the variation of stresses around the borehole does not disturb the pore pressure field. Hence, the solution is obtained as:

$$\sigma_{rr}^{(1)} = \mathrm{H}(t)(P_0 - p_w)\frac{R^2}{r^2} \tag{60a}$$

$$\sigma_{\theta\theta}^{(1)} = -\mathrm{H}(t)(P_0 - p_w)\frac{R^2}{r^2} \tag{60b}$$

$$p^{(1)} = 0. \tag{60c}$$

For Mode 2, $p^{(2)}$ can be obtained from the diffusion eqn (57); however, it can be solved analytically only in the Laplace transform domain. $p^{(2)}$, $\sigma_{rr}^{(2)}$, and $\sigma_{\theta\theta}^{(2)}$ are given below as their Laplace transforms:

$$\tilde{p}^{(2)} = -\frac{p_0 - p_i}{s}\frac{\mathrm{K}_0(\xi)}{\mathrm{K}_0(\beta)} \tag{61a}$$

$$\tilde{\sigma}_{rr}^{(2)} = -\frac{p_0 - p_i}{s}\frac{2G\alpha}{M_{11}}\left[\frac{R}{r}\frac{\mathrm{K}_1(\xi)}{\beta\mathrm{K}_0(\beta)} - \frac{R^2}{r^2}\frac{\mathrm{K}_1(\beta)}{\beta\mathrm{K}_0(\beta)}\right] \tag{61b}$$

$$\tilde{\sigma}_{\theta\theta}^{(2)} = \frac{p_0 - p_i}{s}\frac{2G\alpha}{M_{11}}\left[\frac{R}{r}\frac{\mathrm{K}_1(\xi)}{\beta\mathrm{K}_0(\beta)} - \frac{R^2}{r^2}\frac{\mathrm{K}_1(\beta)}{\beta\mathrm{K}_0(\beta)} + \frac{\mathrm{K}_0(\xi)}{\mathrm{K}_0(\beta)}\right] \tag{61c}$$

where $\mathrm{K}_n$ denotes the modified Bessel function of the second kind of order $n$.

Again, Mode 3 can only be solved analytically in the Laplace transform domain. From the equilibrium eqns (6), the constitutive eqns (1) and (3), as well as the strain–displacement relationship (7), the Navier's equation in cylindrical coordinate system can be obtained as:

$$M_{11}\frac{\partial\varepsilon}{\partial r} - 2G\frac{1}{r}\frac{\partial\omega}{\partial\theta} - \alpha\frac{\partial p}{\partial r} = 0 \tag{62a}$$

$$M_{11}\frac{1}{r}\frac{\partial\varepsilon}{\partial\theta} + 2G\frac{\partial\omega}{\partial r} - \alpha\frac{1}{r}\frac{\partial p}{\partial\theta} = 0 \tag{62b}$$

where

$$\omega = \frac{1}{2}\left(\frac{1}{r}\frac{\partial(ru_\theta)}{\partial r} - \frac{1}{r}\frac{\partial u_r}{\partial\theta}\right). \tag{63}$$

Applying the Laplace transform to Navier's eqns (62a), and the diffusion eqn (10) yields:

$$\frac{M_{11}+\alpha^2 M}{2G}\frac{\partial\tilde{\varepsilon}}{\partial r} - \frac{1}{r}\frac{\partial\tilde{\omega}}{\partial\theta} - \frac{\alpha M}{2G}\frac{\partial\tilde{\zeta}}{\partial r} = 0 \tag{64a}$$

$$\frac{M_{11}+\alpha^2 M}{2G}\frac{1}{r}\frac{\partial\tilde{\varepsilon}}{\partial\theta} + \frac{\partial\tilde{\omega}}{\partial r} - \frac{\alpha M}{2G}\frac{1}{r}\frac{\partial\tilde{\zeta}}{\partial\theta} = 0 \tag{64b}$$

$$\frac{\partial^2\tilde{\zeta}}{\partial r^2} + \frac{1}{r}\frac{\partial\tilde{\zeta}}{\partial r} + \frac{1}{r^2}\frac{\partial^2\tilde{\zeta}}{\partial\theta^2} - \frac{s}{c_T}\tilde{\zeta} = 0. \tag{64c}$$

In view of the asymmetry of Mode 3, it can be assumed that:

$$(\tilde{\zeta}^{(3)}, \tilde{\varepsilon}^{(3)}, \tilde{u}_r^{(3)}, \tilde{\sigma}_r^{(3)}, \tilde{\sigma}_\theta^{(3)}, \tilde{p}^{(3)}) = (\tilde{Z}, \tilde{E}, \tilde{U}_r, \tilde{S}_r, \tilde{S}_\theta, \tilde{P})\cos 2(\theta - \theta_r) \tag{65a}$$

$$(\tilde{\omega}^{(3)}, \tilde{u}_\theta^{(3)}, \tilde{\tau}_{r\theta}^{(3)}) = (\tilde{W}, \tilde{U}_\theta, \tilde{S}_{r\theta})\sin 2(\theta - \theta_r). \tag{65b}$$

Substituting relations (65) into eqns (64), a set of ordinary differential equations is produced. They are:

$$\frac{M_{11}+\alpha^2 M}{2G}\frac{\mathrm{d}\tilde{E}}{\mathrm{d}r}-2\frac{\tilde{W}}{r}-\frac{\alpha M}{2G}\frac{\mathrm{d}\tilde{Z}}{\mathrm{d}r}=0 \tag{66a}$$

$$\frac{M_{11}+\alpha^2 M}{2G}\frac{\tilde{E}}{r}-\frac{1}{2}\frac{\mathrm{d}\tilde{W}}{\mathrm{d}r}-\frac{\alpha M}{2G}\frac{\tilde{Z}}{r}=0 \tag{66b}$$

$$\frac{\mathrm{d}^2\tilde{Z}}{\mathrm{d}r^2}+\frac{1}{r}\frac{\mathrm{d}\tilde{Z}}{\mathrm{d}r}-\left(\frac{s}{c_T}r^2+4\right)\tilde{Z}=0. \tag{66c}$$

Solving the above set of ordinary differential eqns (66) with associated boundary conditions, the following expressions are obtained:

$$\tilde{p}^{(3)}=\cos 2(\theta-\theta_r)\frac{S_0}{s}\left[\frac{c_T}{2G\kappa}C_1\mathrm{K}_2(\xi)+A_1C_2\frac{R^2}{r^2}\right] \tag{67a}$$

$$\tilde{\sigma}_{rr}^{(3)}=\cos 2(\theta-\theta_r)\frac{S_0}{s}\left[A_1C_1\left(\frac{1}{\xi}\mathrm{K}_1(\xi)+\frac{6}{\xi^2}\mathrm{K}_2(\xi)\right)-A_2C_2\frac{R^2}{r^2}-3C_3\frac{R^4}{r^4}\right] \tag{67b}$$

$$\tilde{\sigma}_{\theta\theta}^{(3)}=\cos 2(\theta-\theta_r)\frac{S_0}{s}\left\{-A_1C_1\left[\frac{1}{\xi}\mathrm{K}_1(\xi)+\left(1+\frac{6}{\xi^2}\right)\mathrm{K}_2(\xi)\right]+3C_3\frac{R^4}{r^4}\right\} \tag{67c}$$

$$\tilde{\tau}_{r\theta}^{(3)}=\sin 2(\theta-\theta_r)\frac{S_0}{s}\left[2A_1C_1\left(\frac{1}{\xi}\mathrm{K}_1(\xi)\right.\right. \tag{67d}$$

$$\left.\left.+\frac{3}{\xi^2}\mathrm{K}_2(\xi)\right)-\frac{A_2}{2}C_2\frac{R^2}{r^2}-3C_3\frac{R^4}{r^4}\right] \tag{67e}$$

where

$$C_1=\frac{4}{2A_1(M_3-M_2)-A_2M_1} \tag{68a}$$

$$C_2=-\frac{4M_1}{2A_1(M_3-M_2)-A_2M_1} \tag{68b}$$

$$C_3=\frac{2A_1(M_2+M_3)+3A_2M_1}{3[2A_1(M_3-M_2)-A_2M_1]}. \tag{68c}$$

In the above,

$$A_1=\frac{\alpha M}{M_{11}+\alpha^2 M} \tag{69a}$$

$$A_2=\frac{M_{11}+M_{12}+2\alpha^2 M}{M_{11}+\alpha^2 M} \tag{69b}$$

$$M_1=\frac{M_{11}}{2G\alpha}\mathrm{K}_2(\beta) \tag{69c}$$

$$M_2=\frac{1}{\beta}\mathrm{K}_1(\beta)+\frac{6}{\beta^2}\mathrm{K}_2(\beta) \tag{69d}$$

$$M_3=2\left(\frac{1}{\beta}\mathrm{K}_1(\beta)+\frac{3}{\beta^2}\mathrm{K}_2(\beta)\right). \tag{69e}$$

To evaluate $\sigma_{rr}^{(2)}$, $\sigma_{rr}^{(3)}$, $\sigma_{\theta\theta}^{(2)}$, $\sigma_{\theta\theta}^{(3)}$, $\tau_{r\theta}^{(3)}$, $p^{(2)}$, and $p^{(3)}$ in the time domain, a numerical technique for the inverse of the Laplace transform should be applied.